

# SCIENTIFIC REPORTS

OPEN

## Duplication events downstream of *IRX1* cause North Carolina macular dystrophy at the MCDR3 locus

Valentina Cipriani<sup>1,2,3</sup>, Raquel S. Silva<sup>1,2</sup>, Gavin Arno<sup>1,2</sup>, Nikolas Pontikos<sup>1,3</sup>, Ambreen Kalhoro<sup>1,2</sup>, Sandra Valeina<sup>4</sup>, Inna Inashkina<sup>5</sup>, Mareta Audere<sup>5,6</sup>, Katrina Rutka<sup>5,6</sup>, Bernard Puech<sup>7</sup>, Michel Michaelides<sup>1,2</sup>, Veronica van Heyningen<sup>1</sup>, Baiba Lace<sup>5,8</sup>, Andrew R. Webster<sup>1,2</sup> & Anthony T. Moore<sup>1,2,9</sup>

Autosomal dominant North Carolina macular dystrophy (NCMD) is believed to represent a failure of macular development. The disorder has been linked to two loci, MCDR1 (chromosome 6q16) and MCDR3 (chromosome 5p15-p13). Recently, non-coding variants upstream of *PRDM13* (MCDR1) and a duplication including *IRX1* (MCDR3) have been identified. However, the underlying disease-causing mechanism remains uncertain. Through a combination of sequencing studies on eighteen NCMD families, we report two novel overlapping duplications at the MCDR3 locus, in a gene desert downstream of *IRX1* and upstream of *ADAMTS16*. One duplication of 43 kb was identified in nine families (with evidence for a shared ancestral haplotype), and another one of 45 kb was found in a single family. Three families carry the previously reported V2 variant (MCDR1), while five remain unsolved. The MCDR3 locus is thus refined to a shared region of 39 kb that contains DNase hypersensitive sites active at a restricted time window during retinal development. Publicly available data confirmed expression of *IRX1* and *ADAMTS16* in human fetal retina, with *IRX1* preferentially expressed in fetal macula. These findings represent a major advance in our understanding of the molecular genetics of NCMD and provide insights into the genetic pathways involved in human macular development.

North Carolina macular dystrophy (NCMD) is a rare autosomal dominant disorder in which there is abnormal development of the macula, a crucial structure of the central retina responsible for central vision and colour perception<sup>1</sup>. Understanding the genetics of rare developmental macular conditions is key for unravelling the mechanism of development of this structure that is found only in higher primates within mammals<sup>1</sup>. NCMD shows fully penetrant inheritance and is considered a non-progressive disorder with a wide range of phenotypic manifestations, usually affecting both eyes symmetrically<sup>2,3</sup>. Phenotypic presentation varies from mild cases with drusen-like deposits covering the macular region but with little or no visual impairment, to severe cases with marked central chorioretinal atrophy and poor vision. Although generally non-progressive, complications associated with choroidal neovascularization can contribute to visual deterioration.

The molecular genetics of NCMD has been extensively investigated with the disorder being mapped to chromosome 6q16 (MCDR1, MIM:136550) in multiple families of different ethnic origins since the early 1990s<sup>4-10</sup>. A similar phenotype has been assigned to a second locus at 5p15-p13 (MCDR3, MIM:608850)<sup>3,11</sup>. Interestingly, several studies reported evidence for ancestral haplotypes at the MCDR1 locus<sup>2,12,13</sup>. Early sequencing studies of the two disease intervals failed to identify exonic disease-causing variants<sup>2,14</sup>. More recently, three novel single nucleotide variants (SNVs) were identified in 11 families at the MCDR1 locus, within a DNaseI hypersensitivity site (DHS), in the non-coding interval between *PRDM13* and the neighbouring overlapping genes *CCNC/TSTD3*<sup>15</sup>. Two tandem duplications including the full coding region of *PRDM13*, with some additional upstream and

<sup>1</sup>UCL Institute of Ophthalmology, London, UK. <sup>2</sup>Moorfields Eye Hospital, London, UK. <sup>3</sup>UCL Genetics Institute, London, UK. <sup>4</sup>Children's Clinical University Hospital, Riga, Latvia. <sup>5</sup>Latvian Biomedical Research and Study Centre, Riga, Latvia. <sup>6</sup>Riga Stradins University, Riga, Latvia. <sup>7</sup>Exploration de la Vision et Neuro-Ophthalmologie, Centre Hospitalier Universitaire, Lille, France. <sup>8</sup>Centre Hospitalier de l'Université Laval, Québec, Canada. <sup>9</sup>Ophthalmology Department, UCSF School of Medicine, San Francisco, CA, USA. Valentina Cipriani and Raquel S. Silva contributed equally to this work. Correspondence and requests for materials should be addressed to V.C. (email: [v.cipriani@ucl.ac.uk](mailto:v.cipriani@ucl.ac.uk)) or A.R.W. (email: [andrew.webster@ucl.ac.uk](mailto:andrew.webster@ucl.ac.uk)) or A.T.M. (email: [tony.moore@ucsf.edu](mailto:tony.moore@ucsf.edu))

Family number	Family ID	Origin	Phenotype	Experimental procedure	Causative allele change	Nucleotide change	Number of affected family members analysed	Number of unaffected family members analysed	Total number of family members analysed
1	GC19806 <sup>14</sup>	Latvian	NCMD	SNP, aCGH, WGS, PCR/Sanger	chr5:4391377–4436535	45158 bp duplication	5	1	6
2	GC15626 <sup>11</sup>	British	NCMD	SNP, aCGH, WGS, PCR/Sanger	chr5:4396927–4440442	43515 bp duplication	9	8	17
3	GC15119	British	NCMD	SNP, aCGH, WGS, PCR/Sanger	chr5:4396927–4440442	43515 bp duplication	4	0	4
4	GC13840	British	NCMD	SNP, WGS, PCR/Sanger	chr5:4396927–4440442	43515 bp duplication	3	0	3
5	GC19075	British	NCMD	SNP, WGS, PCR/Sanger	chr5:4396927–4440442	43515 bp duplication	3	0	3
6	GC15475	British	NCMD	SNP, WGS, PCR/Sanger	chr5:4396927–4440442	43515 bp duplication	1	0	1
7	GC11709	British	NCMD	SNP, WGS, PCR/Sanger	chr5:4396927–4440442	43515 bp duplication	1	0	1
8	GC16913	British	NCMD	PCR/Sanger	chr5:4396927–4440442	43515 bp duplication	1	0	1
9	GC4092	British	NCMD	PCR/Sanger	chr5:4396927–4440442	43515 bp duplication	1	0	1
10	GC23501	British	NCMD	PCR/Sanger	chr5:4396927–4440442	43515 bp duplication	2	1	3
11	GC15416	British	NCMD	SNP, PCR/Sanger	chr6:100040987	G > C (V2)	2	0	2
12	GC3722 <sup>7</sup>	British	NCMD	SNP, PCR/Sanger	chr6:100040987	G > C (V2)	12	8	20
13	GC17225 <sup>9,15</sup>	French	NCMD	SNP, PCR/Sanger	chr6:100040987	G > C (V2)	12	15	27
						<b>Total</b>	<b>56</b>	<b>33</b>	<b>89</b>

**Table 1.** Summary of families with two newly reported tandem duplications at the MCDR3 locus and previously identified V2 variant at the MCDR1 locus. Genomic coordinates refer to GRCh37/hg19 assembly. SNP, aCGH, WGS, PCR/Sanger indicate Illumina SNP array, array-based comparative genomic hybridization, whole-genome sequencing and Sanger Sequencing, respectively. Five affected members from five additional NCMD families were also tested for the presence of previously reported SNVs V1–V3<sup>15</sup> and the two tandem duplications found in this study, but none of these affected individuals was found to carry any of the variants.

downstream sequence included, were also identified<sup>15,16</sup>. One MCDR3-linked family of Danish origin<sup>3</sup> was found to carry a 900 kb tandem duplication<sup>15</sup> that includes the entire coding sequence of *IRX1*. However, duplications of *IRX1* have been observed in several normal individuals from the Database of Genome Variants<sup>15,17</sup> and the significance of this reported variant is uncertain. Thus, the causative mechanism at the 5p15-p13 NCMD locus remains unclear.

In this report we present a combination of genomic investigations in a cohort of 18 NCMD families. The aim of this study was to identify any causative molecular changes and mechanism of disease in these families.

## Results

**Families and brief clinical phenotype description.** Eighteen families with phenotypes consistent with a diagnosis of NCMD were included in the study (Table 1 and Supplementary Fig. S1). Four families were previously reported: suggestive linkage at the MCDR3 locus has been recently described for family 1<sup>14</sup>, family 2 was originally reported to be linked to the MCDR3 locus<sup>11</sup>, and families 12 and 13 were linked to MCDR1<sup>7,9</sup>, with family 13 recently found to carry the SNV V2 upstream of *PRDM13*<sup>15</sup>. All families (mostly of small size) showed autosomal dominant inheritance and had at least one individual with Grade 3 disease. DNA samples from a total of 56 affected and 33 unaffected family members were available for genetic analysis.

Figure 1 shows fundus autofluorescence and optical coherence tomography (OCT) images for selected individuals from families 2 and 3. Individual IV:5 from family 2 presents with a well demarcated, relatively symmetrical, bilateral area of macular chorioretinal atrophy, while individual IV:3 from family 3 shows a mild form of disease with relatively symmetrical, bilateral hyperfluorescent drusen-like deposits concentrated in the macular region.

**Haplotype sharing analysis can exclude or suggest genetic mapping at known NCMD loci.** Haplotype sharing analysis was carried out using the Homozygosity Haplotype (HH) method<sup>18</sup> to search for shared identical-by-descent (IBD) chromosomal segments among affected individuals within each family. This analysis was performed in those families for which Illumina single-nucleotide polymorphism (SNP) array data were available for more than one affected family member (families 1–5 and 12–13). The 6q16 MCDR1 locus was excluded in four families, including the two previously MCDR3-linked families 1<sup>14</sup> and 2<sup>11</sup> and unreported families 3 and 4 (Supplementary Figs S2–S5). Family 5 showed evidence for haplotype sharing at many regions across the genome, including both the 6q16 and 5p15-p13 loci (Supplementary Fig. S6). The two previously reported MCDR1-linked families 12<sup>7</sup> and 13<sup>9</sup> were confirmed with evidence for a Region with a Conserved HH (RCHH) at the 6q16 locus, and not at the 5p15-p13 locus (Supplementary Figs S7–S8).

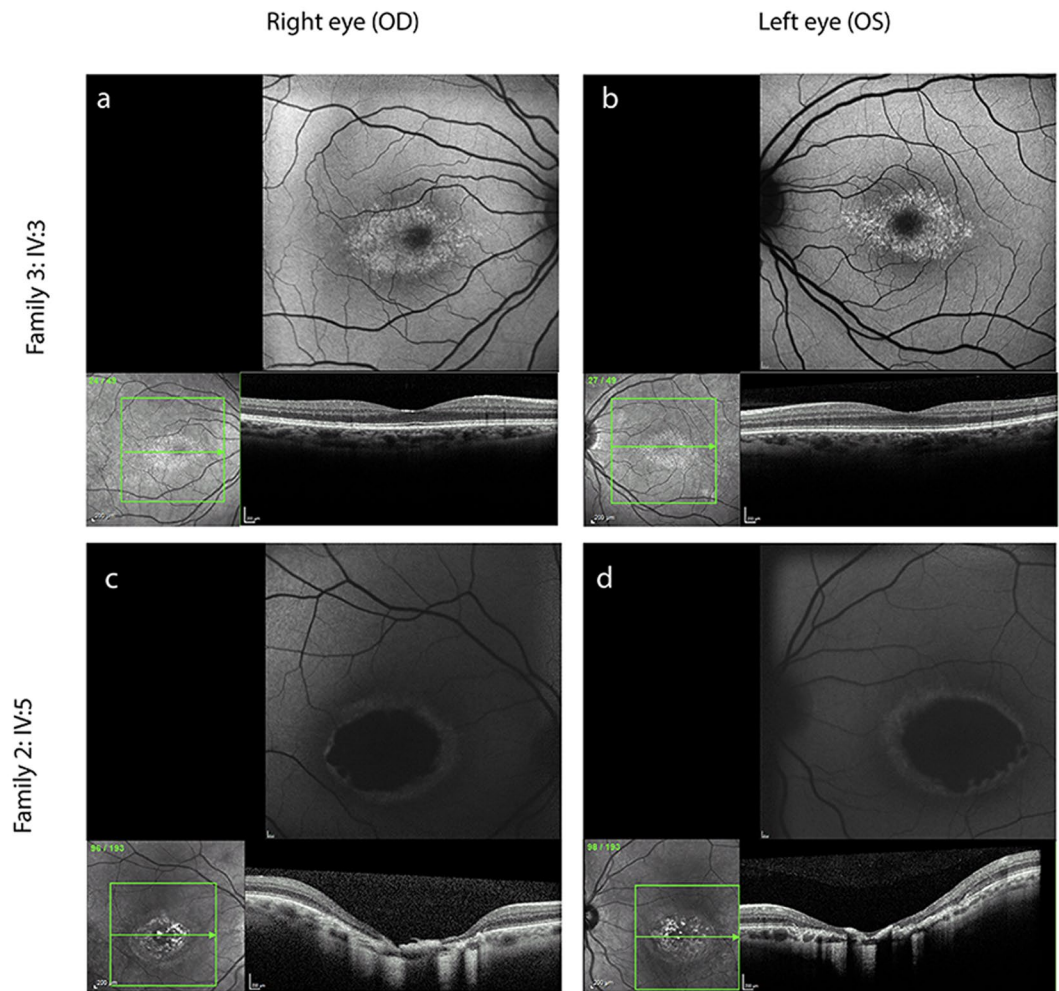


**Figure 1.** NCMD typical clinical presentation in two selected individuals from family 3 (IV:3) and family 2 (IV:5). Each panel shows fundus autofluorescence and optical coherence tomography (OCT) images. Individual IV:3 (a,b) from family 3 shows a mild form of disease with relatively symmetrical, bilateral hyperfluorescent drusen-like deposits concentrated within the macular region and an otherwise normal OCT. Individual IV:5 (c,d) from family 2 presents with a well demarcated, relatively symmetrical and bilateral area of macular chorioretinal atrophy.

**Two additional NCMD families shown to carry previously reported SNV upstream of *PRDM13* at the *MCDR1* locus.** All families, except families 1–4 for which linkage at the 6q16 locus had been excluded via haplotype sharing analysis, were tested with Sanger Sequencing for the three previously reported SNVs (V1–V3) upstream of *PRDM13*<sup>15</sup>. In addition to the previously reported V2 family 13<sup>15</sup>, two more NCMD families were found to harbour the variant V2 (family 11 and the previously described *MCDR1*-linked family 12<sup>7</sup>).

**Array-based comparative genomic hybridization (aCGH) uncovers duplications at the *MCDR3* locus in three NCMD families.** To investigate the *MCDR3* locus for the presence of structural variants (SVs), an aCGH experiment using 10,000 probes spanning the region at chr5:11882–10140073 (GRCh37/hg19) was performed in three affected individuals from families 1–3 which did not show linkage at the 6q16 locus (Supplementary Figs S2–S4). All three families were found to harbour heterozygous duplications of approximately 45 kb, downstream of *IRX1* and upstream of *ADAMTS16* (Fig. 2a). The duplications were found to be located in the minimal overlapping regions chr5:4391880–4434888 (GRCh37/hg19) in family 1 and chr5:4397221–4440150 (GRCh37/hg19) in families 2 and 3. These SVs were not seen in 16 control individuals included in the same aCGH experiment, nor were they present in whole genome sequencing (WGS) data from 650 individuals with inherited retinal disease<sup>19</sup> or in publicly available population copy number variant (CNV) data (CNV browser)<sup>20</sup>.

**WGS identifies four more NCMD families with duplications at the *MCDR3* locus.** Thirteen affected individuals from families 1–7 underwent WGS. Graphical visualisation of individual paired-end reads using Integrative Genomics Viewer (IGV)<sup>21,22</sup> confirmed the presence of heterozygous tandem duplications in families 1–3 (Fig. 2b). Precise breakpoint coordinates were identified from coverage changes, split reads and

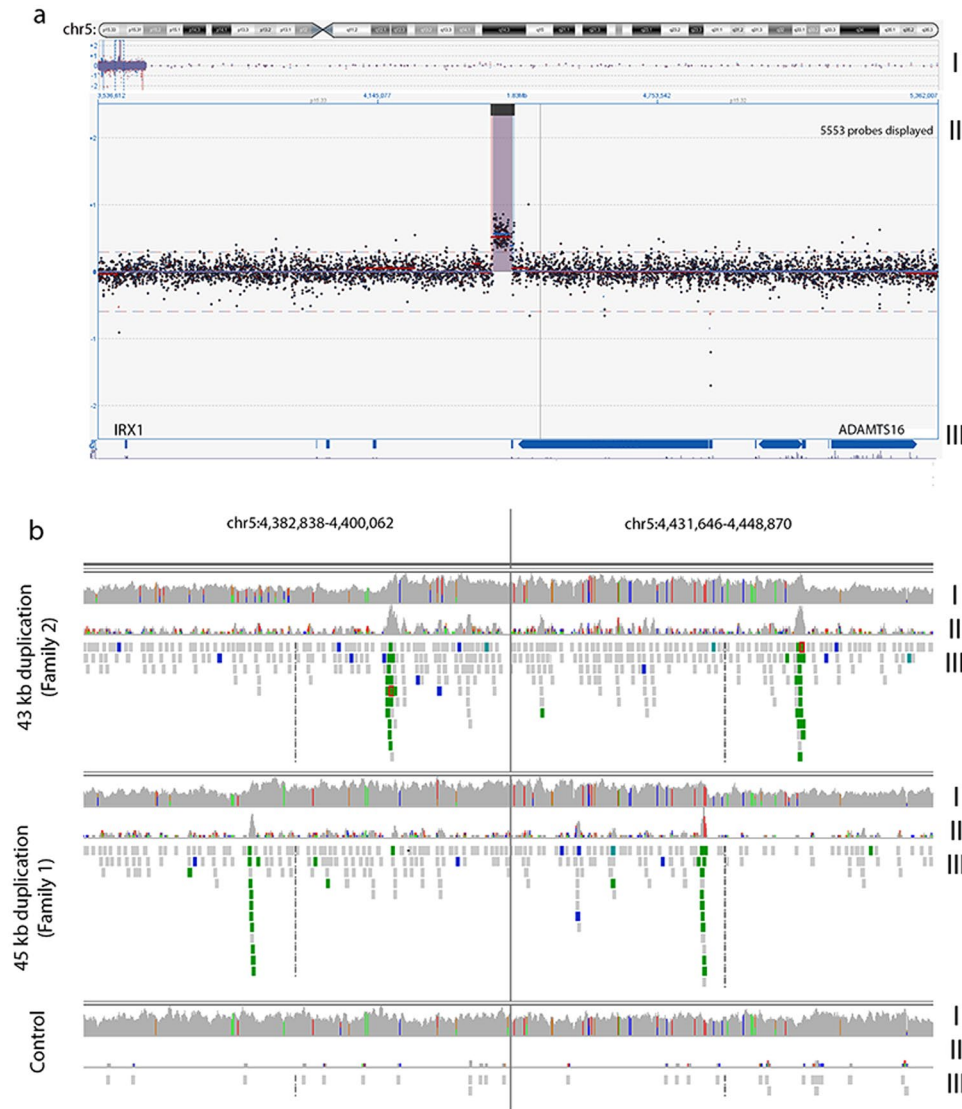


**Figure 2.** NCMD is caused by intergenic duplication events located between *IRX1* and *ADAMTS16*. (a) aCGH experiment (10,000 probes spanning the MCDR3 locus at GRCh37/hg19 chr5:11882–10140073, panel I) performed in three affected individuals from families 1–3 that were found to harbour heterozygous duplications of approximately 43 kb (panel II) located in a gene desert downstream of *IRX1* and upstream of *ADAMTS16* (panel III), also confirmed by WGS (b) by changes in coverage from concordant and discordant reads (panel I and II, respectively) and identification of chimeric reads, pair-reads with opposing orientation (displayed in green, panel III). Panels are presented with a split view option within IGV. The duplications are located in the overlapping regions GRCh37/hg19 chr5:4391880–4434888 (family 1) and GRCh37/hg19 chr5:4397221–4440150 (families 2 and 3).

chimeric reads. Family 1 had a 45158 bp duplicated region (GRCh37/hg19 chr5:4391377–4436535) and families 2 and 3 shared an identical 43515 bp tandem duplication (GRCh37/hg19 chr5:4396927–4440442), overlapping the first identified SV by 85% of the sequence (GRCh37/hg19 chr5:4396925–4436534). Subsequently, members from families 4–7 were also found to carry the same 43 kb duplication.

Polymerase chain reaction (PCR) primers were designed to amplify the novel sequence across the breakpoint between duplicated copies (Table 2, Fig. 3) and used to confirm the predicted breakpoints and assess segregation of the two variants in all available affected and unaffected members of families 1 and 2 (Fig. 3, Table 1 and Supplementary Fig. S1). PCR was then used to genotype the available affected individuals from families 3–7 and confirmed the presence of a band in all affected individuals tested (Table 1 and Supplementary Fig. S1).

**Genotyping reveals three additional previously unmapped NCMD families with duplications at the MCDR3 locus.** The remaining 8 unmapped families were tested with the established PCR assay for both duplications, and 3 of them (families 8–10) were also found to carry the 43 kb duplication (Table 1 and



Duplication size	Primer sequence	T <sub>m</sub> (°C)	Length (bp)
43 kb	F 5'-TTGTGGACTGAGCAAGCAAG-3'	63	532
	R 5'-GGAGCAGAAGTTAAATGTGGAGA-3'		
45 kb	F 5'-TTGCTTGATCAATTCTGCTG-3'	63	500
	R 5'-TTCTCAGTTGGAAGAGCACAAA-3'		

**Table 2.** Primer sequences used for the segregation analysis of the two novel MCDR3 duplications identified in the study. T<sub>m</sub> = Temperature of melting.

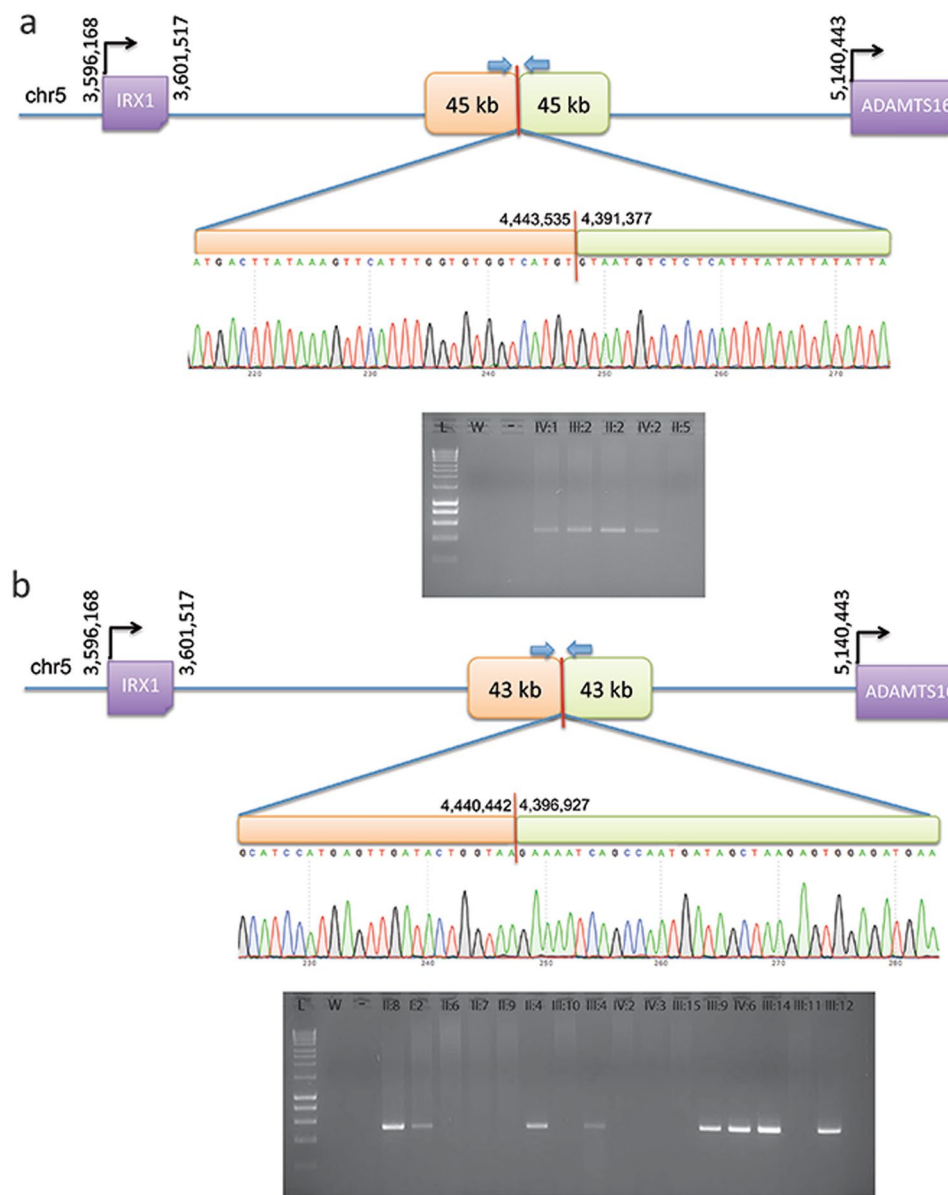


**Figure 3.** PCR and Sanger sequencing validation of duplication breakpoints and segregation in family 1 (a) and family 2 (b). All available individuals (Supplementary Fig. S1) were tested with primers designed across the predicted breakpoints to generate a unique junction fragment sequence. The exact breakpoint is marked with a red bar; PCR primers are represented with blue arrows. L = ladder; W = water; “-” = genomic DNA pooled from control individuals.

Supplementary Fig. S1). Thus, a total of 9 not knowingly related families were shown to harbour the same 43 kb tandem duplication at the MCDR3 locus. Five affected members available from the remaining 5 families did not carry either of the two novel duplications.

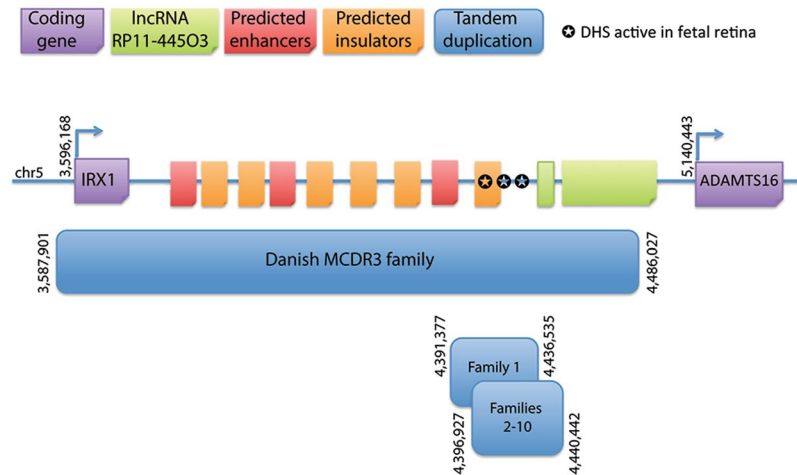


**Figure 4.** Schematic representation of the MCDR3 locus which is refined to a 39 kb shared genomic region (GRCh37/hg19 chr5:4396925–4436534). The shared sequence between a previously reported duplication and the two novel SVs identified in this study is located in a large gene desert, downstream of *IRX1* and upstream of *ADAMTS16*, 800 kb and 693.9 kb from their respective transcription start sites. Publicly available NGS datasets were queried for informative data on chromatin accessibility and 3 sites were found active from human gestation day 72 to 105 in fetal retina, suggestive of functional acting elements within this site.

### Haplotype sharing analysis suggests presence of ancestral haplotypes at the MCDR1 and MCDR3 loci.

We hypothesized that finding the same 6q16 SNV and 5p15 duplication with identical breakpoint in 3 and 9 families respectively, could be due to two different shared ancestral haplotypes suggestive of a common founder, in keeping with previous reports on other 6q16 NCMD families<sup>5, 12, 13, 15</sup>. Therefore, haplotype sharing analysis was performed using available Illumina SNP array data from 14 affected individuals in 3 families carrying the 6q16 V2 variant (families 11–13) and 14 affected individuals in 6 families carrying the 5p15 43 kb duplication (families 2–7). Using a cut-off of 2.0 cM and 2.5 cM respectively, the results confirmed that all the genotyped 6q16 individuals collectively shared a RCHH of approximately 2.5 Mb from GRCh37/hg19 coordinate chr6:98962591 (rs150396) to chr6:101468591 (rs1321204) at the MCDR1 locus, and all the genotyped 5p15 individuals collectively shared a RCHH of approximately 0.9 Mb from GRCh37/hg19 coordinate chr5:4327455 (rs155354) to chr5:5210050 (rs1560063) at the MCDR3 locus (Supplementary Tables S1–S2 and Supplementary Figs S9–S10).

### Discussion

We report two distinct heterozygous tandem duplications at the MCDR3 locus in 30 affected individuals from 10 NCMD families. The two novel SVs overlap the previously described duplication found in a single NCMD family of Danish origin<sup>15</sup> and further refine the 5p15 NCMD locus to a shared region of 39 kb in a gene desert downstream of *IRX1* and upstream of *ADAMTS16* (800 kb and 693.9 kb from the respective transcription start sites, Fig. 4).

We postulated that the 39 kb shared region could harbour *cis*-acting elements that contribute to the fine tuning of gene expression during macular development, affecting target gene expression spatially, temporally and/or quantitatively. Publicly available platforms were queried for informative data on gene expression and chromatin accessibility in relevant tissue types. A dataset screening for gene expression in fetal retina confirmed high expression of *IRX1* at 19–20 weeks of gestation in the macula, and medium expression levels in other regions (Supplementary Fig. S11). In contrast, *ADAMTS16* had medium expression levels throughout the retina<sup>23, 24</sup>. Although no role in retinal pathophysiology has been described for *ADAMTS16*, the gene has high sequence similarity to *ADAMTS18* which has been previously associated with retinal disease<sup>25</sup>. Overall, the data suggest that the pattern and/or refined spatial dosage and timing of expression of the transcription factor *IRX1* may be important in macular development. A second dataset provided information on open chromatin conformation using DNase-accessible sequencing in fetal retina tissues at 5 stages from gestation day 72 to 125 (~10 to 18 weeks)<sup>26</sup>. Different sites were identified to be open/active within the 39 kb shared region at four out of five time points (~10–15 weeks of gestation) available during retinal development (Table 3). Interestingly, one of the sites was active during three developmental stages and the remaining four sites were functionally active as two overlapping pairs. At the last time point (day 125, ~18 weeks), all sites were inactive/closed. In the context of human macular development, the sites are active during the period where retinal progenitor cells are proliferating and differentiating towards photoreceptor fate<sup>27</sup>; by week 14 of gestation, cells of the central retina exit mitosis<sup>27</sup>, corresponding to the period where DHSs are turning off.

As mentioned, the MCDR1 locus on chromosome 6q16 is associated with variants sited within a DHS, which suggests that aspects of macular development may be highly gene dosage sensitive. Exploring the function and precise target of such regulatory domains in both loci will be essential for understanding the disease mechanism of NCMD and investigating its potential role in the context of normal macular development. The graded

Chromosome	Start position	End position	Gestation day (fetal retina)
5	4418340	4418490	74
5	4420820	4420970	74, 89, 103
5	4418320	4418470	85
5	4420860	4421010	85
5	4409260	4409410	103

**Table 3.** DHSs active during fetal retina development at the 39 kb shared duplicated region (GRCh37/hg19 chr5:4396925–4436534). Gestation day 125 shows no active site at the 39 kb shared region. The fetal retina datasets were available from ENCODE<sup>26</sup>, produced by the Stamatoyannopoulos' laboratory.

expression of *IRX1* and known involvement in retinal development<sup>28, 29</sup>, but not *ADAMTS16* in the macular region, suggests that *IRX1* is the probable target of the putative retinal regulatory element which, when duplicated, may cause misregulation of *IRX1*.

Eye development, like other organogenesis processes, requires the precise spatio-temporal and quantitative expression of genes, orchestrated by a complex network of regulatory mechanisms influencing critical transcription factors and other developmental genes. The lack of readily accessible animal or *in vitro* models has hindered detailed understanding of macular development, as this structure only evolved in higher primates among mammals. Recently, disrupted developmental expression of the transcription factor and histone methyltransferase *PRDM13*<sup>30, 31</sup> was suggested as a disease mechanism for NCMD at the 6q16 locus, based on the identification of non-coding SNVs and duplication events residing in an overlapping region upstream of *PRDM13* in many MCDR1 families. Differential regulation of *PRDM13* in eyecups derived from wild-type induced pluripotent stem cells (iPSCs)<sup>15, 16</sup> was suggested. However, no causal relationship between the non-coding variants and *PRDM13* expression has been identified.

Despite variable presentation in affected individuals, the NCMD phenotypic spectrum is indistinguishable in patients assigned to either of the two linked loci, MCDR1 and MCDR3. Whether a biological and functional connection between *PRDM13* at the MCDR1 locus and the most likely candidate gene *IRX1* at the MCDR3 locus exists warrants further investigation. iPSC technology and CRISPR manipulation in eye cups from normal and affected individuals may help elucidate the molecular mechanism<sup>32, 33</sup> and the potential molecular links between the two genes. Importantly, the involvement of ancestral variation at both the 6q16 and 5p15 loci (Supplementary Tables S1–S2 and Supplementary Figs S9–S10) in such a highly penetrant dominant disease is intriguing, with the implication that there may exist a significant number of unrecognized related NCMD families. Full clinical examination reveals a high degree of penetrance, but visually unaffected individuals in whole families may fail to be ascertained.

Finally, the two novel duplications identified in this study significantly further the understanding of the molecular genetics of NCMD at the MCDR3 locus and provide additional effective tools for the molecular diagnosis of NCMD families.

## Materials and Methods

**Families.** All families were ascertained at Moorfields Eye Hospital, London, United Kingdom, except for family 1<sup>14</sup> (Vision Centre, Children's Clinical University Hospital, Riga, Latvia) and family 13<sup>9</sup> (Centre Hospitalier Régional Universitaire de Lille, France). When possible, retinal imaging was undertaken using colour fundus photography, fundus autofluorescence and OCT imaging. Blood/saliva samples were collected for DNA extraction, genotyping and sequence analyses. The study protocol was approved by the local ethics committees (Central Medical Ethics Committee of Latvian Republic; NRES Committee London – Camden & Islington) and conformed to the tenets of the Declaration of Helsinki. Written informed consent was obtained from all participants, or their parents, before inclusion in the study.

**Genotyping.** Genomic DNA was extracted from whole blood/saliva and genotyped using the Illumina HumanOmniExpress-24 v1.0 beadchip (Illumina, Inc., San Diego, CA, USA). Genotypes were determined using the Genotyping Module in the Illumina GenomeStudio v2011.1 software.

**Haplotype sharing analysis.** In order to search for chromosomal segments sharing the same haplotype across affected individuals (within the same family or across different families), the non-parametric HH method<sup>18</sup> was used for the analysis of those affected individuals that were genotyped with the Illumina array. The HH is a type of haplotype described by the homozygous SNPs only (all heterozygous SNPs are removed) and, therefore, can be uniquely determined on each chromosome. Since affected family members who inherited the same mutation from a common ancestor share a chromosomal segment IBD around the disease gene, they should not have discordant homozygous calls in the IBD region and thus they should share the same HH. The HH approach predicts IBD regions through the identification of RCHs defined as those regions with a shared HH among affected individuals and a genetic length longer than a certain cut-off value (recommended cut-off for Illumina HumanOmniExpress array is 2.5/3.0 cM for the analysis of one single family).

**aCGH.** aCGH was performed at Oxford Gene Technology (OGT) (Begbroke, United Kingdom) using a custom design consisting of 10,000 probes spanning the MCDR3 locus at GRCh37/hg19 chr5:11882–10140073 (approximately 1 probe every 1,000 bp), designed with Agilent e-Array software (Agilent Technologies Inc., Santa Clara, CA, USA), in three individuals from families 1–3 (Supplementary Fig. S1). Sixteen other individuals

affected by non-ocular phenotypes were also included in the experiment and used as controls in the analysis. Scanned images of the arrays were processed with OGT CytoSure™ Interpret Software v4.4 using the Accelerate Workflow for calling CNVs. Duplications or deletions were considered when the  $\log_2$  ratio of the Cy3/Cy5 intensities of a region encompassing at least four probes was  $> 0.3$  or  $< -0.6$ , respectively (software default settings).

**WGS and bioinformatics analysis.** WGS was performed using the Illumina HiSeq X10 platform (Illumina, Inc., San Diego, CA, USA), generating minimum coverage of 30X. Reads were aligned to the hg19 human reference sequence (build GRCh37) with novoalign (version 3.02.08). The aligned reads were sorted by base pair position and duplicates were marked using novosort. Discordant reads were marked with samblaster (version 0.1.20) and sent to a separate file for manual inspection of breakpoints using the IGV (version 2.3.61). SVs were manually investigated using the IGV by identifying peaks of discordant reads which were interpreted as breakpoints. The identified duplicated regions were also screened for the presence of common copy number variants using data from the CNV browser<sup>20</sup> ([https://personal.broadinstitute.org/handsake/mcnv\\_data/](https://personal.broadinstitute.org/handsake/mcnv_data/)) and WGS data from 650 individuals with inherited retinal disease<sup>19</sup>.

**Sanger sequencing validation of duplication events.** Segregation analysis of the duplication events identified by WGS was performed using primers (Table 2) designed to span the end of first copy and start of second copy. A graphical representation is shown in Fig. 3. After sequence confirmation with Sanger sequencing, PCR was used to genotype selected individuals from all identified families.

**In silico analysis of duplicated sequences and expression of flanking genes.** The Encyclopedia of DNA Elements (ENCODE)<sup>26</sup> was interrogated for fetal retina datasets of interest. Bed files from DNA-seq datasets (ENCFF249FGP, ENCFF937NUZ, ENCFF401BCF, ENCFF591NRB, ENCFF265ZNN, Stamatoyannopoulos' laboratory) were downloaded and investigated at the shared duplicated region with R Studio. A second microarray expression dataset on human fetal retina (19–20 gestation week) was queried for the genes of interest<sup>24</sup> using the platform GENEVESTIGATOR<sup>23</sup>.

**Data availability statement.** The datasets generated during the current study are not publicly available due to limitations imposed by the scope of participant consent, but are available from the corresponding authors on reasonable request.

## References

- Provis, J. M., Dubis, A. M., Maddess, T. & Carroll, J. Progress in Retinal and Eye Research Adaptation of the central retina for high acuity vision: Cones, the fovea and the avascular zone. *Prog. Retin. Eye Res.* **35**, 63–81 (2013).
- Yang, Z. *et al.* Clinical characterization and genetic mapping of North Carolina macular dystrophy. *Vision Research* **48**, 470–477 (2008).
- Rosenberg, T. *et al.* Clinical and genetic characterization of a Danish family with North Carolina macular dystrophy. *Mol. Vis.* **16**, 2659–2668 (2010).
- Small, K. W. *et al.* North Carolina macular dystrophy is assigned to chromosome 6. *Genomics* **13**, 681–685 (1992).
- Pauleikhoff, D. *et al.* Clinical and genetic evidence for autosomal dominant North Carolina macular dystrophy in a German family. *American Journal of Ophthalmology* **124**, 412–415 (1997).
- Rabb, M. F., Mullen, L., Yelchits, S., Udar, N. & Small, K. W. A North Carolina macular dystrophy phenotype in a Belizean family maps to the MCDR1 locus. *Am. J. Ophthalmol.* **125**, 502–8 (1998).
- Reichel, M. B. *et al.* Phenotype of a British North Carolina macular dystrophy family linked to chromosome 6q. *Br. J. Ophthalmol.* **82**, 1162–1168 (1998).
- Rohrschneider, K., Blankenagel, A., Kruse, F. E., Fendrich, T. & Völcker, H. E. Macular function testing in a German pedigree with North Carolina macular dystrophy. *Retina* **18**, 453–9 (1998).
- Small, K. W., Puech, B., Mullen, L. & Yelchits, S. North Carolina macular dystrophy phenotype in France maps to the MCDR1 locus. *Mol. Vis.* **3**, 1 (1997).
- Small, K., Garcia, C., Gallardo, G., Udar, N. & Yelchits, S. North Carolina macular dystrophy (MCDR1) in Texas. *Retina* **18**, 448–452 (1998).
- Michaelides, M. *et al.* An early-onset autosomal dominant macular dystrophy (MCDR3) resembling North Carolina macular dystrophy maps to chromosome 5. *Investig. Ophthalmol. Vis. Sci.* **44**, 2178–2183 (2003).
- Sauer, C. G. *et al.* An ancestral core haplotype defines the critical region harbouring the North Carolina macular dystrophy gene (MCDR1). *J. Med. Genet.* **34**, 961–966 (1997).
- Small, K. W. North Carolina macular dystrophy: clinical features, genealogy, and genetic linkage analysis. *Trans. Am. Ophthalmol. Soc.* **96**, 925–961 (1998).
- Audere, M. *et al.* Genetic linkage studies of a North Carolina macular dystrophy family. *Medicina (Kaunas)*. **52**, 180–186 (2016).
- Small, K. W. *et al.* North Carolina Macular Dystrophy Is Caused by Dysregulation of the Retinal Transcription Factor PRDM13. *Ophthalmology* **123**, 9–18 (2016).
- Bowne, S. J. *et al.* North Carolina macular dystrophy (MCDR1) caused by a novel tandem duplication of the PRDM13 gene. *Mol. Vis.* **22**, 1239–1247 (2016).
- MacDonald, J. R., Ziman, R., Yuen, R. K. C., Feuk, L. & Scherer, S. W. The Database of Genomic Variants: A curated collection of structural variation in the human genome. *Nucleic Acids Res.* **42** (2014).
- Miyazawa, H. *et al.* Homozygosity haplotype allows a genomewide search for the autosomal segments shared among patients. *Am. J. Hum. Genet.* **80**, 1090–102 (2007).
- Carss, K. J. *et al.* Comprehensive Rare Variant Analysis via Whole-Genome Sequencing to Determine the Molecular Pathology of Inherited Retinal Disease. *Am. J. Hum. Genet.* **100**, 75–90 (2017).
- Handsaker, R. E. *et al.* Large multiallelic copy number variations in humans. *Nat. Genet.* **47**, 1–10 (2015).
- Robinson, J. T. *et al.* Integrative genomics viewer. *Nat. Biotechnol.* **29**, 24–26 (2011).
- Thorvaldsdóttir, H., Robinson, J. T. & Mesirov, J. P. Integrative Genomics Viewer (IGV): High-performance genomics data visualization and exploration. *Brief. Bioinform.* **14**, 178–192 (2013).
- Hruz, T. *et al.* Genevestigator V3: A Reference Expression Database for the Meta-Analysis of Transcriptomes. *Adv. Bioinformatics* **2008**, 1–5 (2008).
- Kozulin, P. & Provis, J. M. Differential gene expression in the developing human macula: Microarray analysis using rare tissue samples. *J. Ocul. Biol. Dis. Infor.* **2**, 176–189 (2009).



25. Chandra, A. *et al.* Expansion of ocular phenotypic features associated with mutations in ADAMTS18. *JAMA Ophthalmol.* **132**, 996–1001 (2014).
26. Dunham, I. *et al.* An integrated encyclopedia of DNA elements in the human genome. *Nature* **489**, 57–74 (2012).
27. Provis, J. M., van Driel, D., Billson, F. A. & Russell, P. Development of the human retina: patterns of cell distribution and redistribution in the ganglion cell layer. *J. Comp. Neurol.* **233**, 429–51 (1985).
28. Choy, S. W. *et al.* A cascade of irx1a and irx2a controls shh expression during retinogenesis. *Dev. Dyn.* **239**, 3204–3214 (2010).
29. Cheng, C. W., Yan, C. H. M., Hui, C. C., Strähle, U. & Cheng, S. H. The homeobox gene irx1a is required for the propagation of the neurogenic waves in the zebrafish retina. *Mech. Dev.* **123**, 252–263 (2006).
30. Watanabe, S. *et al.* Prdm13 regulates subtype specification of retinal amacrine interneurons and modulates visual sensitivity. *J. Neurosci.* **35**, 8004–20 (2015).
31. Hanotel, J. *et al.* The Prdm13 histone methyltransferase encoding gene is a Ptf1a-Rbpj downstream target that suppresses glutamatergic and promotes GABAergic neuronal fate in the dorsal neural tube. *Dev. Biol.* **386**, 340–357 (2014).
32. Zhong, X. *et al.* Generation of three-dimensional retinal tissue with functional photoreceptors from human iPSCs. *Nat. Commun.* **5**, 4047 (2014).
33. Schwarz, N. *et al.* Translational read-through of the RP2 Arg120stop mutation in patient iPSC-derived retinal pigment epithelium cells. *Hum. Mol. Genet.* **24**, 972–86 (2015).

## Acknowledgements

The authors would like to acknowledge the ENCODE Consortium and Stamatoyannopoulos' laboratory for generating the DNA-seq datasets queried in this study, the NIHR BioResource - Rare Disease Consortium (Dr. Keren J Carss and Prof. F Lucy Raymond) for access to CNV data from WGS data, Dr. Gabriela E Jones (University Hospitals of Leicester NHS Trust, Leicester, UK) for help with patient recruitment, Dr. Vincent Plagnol (UCL Genetics Institute, London, UK) for access to control aCGH data, and UCL Computer Science Cluster and Technical Support (London, UK). This work was supported by grants from the NIHR Biomedical Research Centre at Moorfields Eye Hospital National Health Service Foundation Trust and UCL Institute of Ophthalmology (London, UK), the Research to Prevent Blindness (USA), the British Eye Research Foundation (UK), Fight for Sight (UK), the Macular Society (UK), Moorfields Eye Hospital Special Trustees (UK), Moorfields Eye Charity (UK), the Foundation Fighting Blindness (USA), the British Heart Foundation (UK) and Retinitis Pigmentosa Fighting Blindness (UK). RSS is funded through a Fight for Sight PhD studentship granted to ARW and VvH. The views expressed in this publication are those of the authors and not necessarily those of the funding bodies.

## Author Contributions

Study conception and design: A.T.M., A.R.W., V.v.H., V.C., R.S.S., G.A. Patient recruitment and phenotyping: A.T.M., A.R.W., A.K., M.M., B.P., B.L., S.V. Acquisition of data: V.C., R.S.S., G.A., I.L., M.A., K.R. Analysis and/or interpretation of data: V.C., R.S.S., N.P., G.A. Drafting of manuscript: V.C., R.S.S. Critical revision for important intellectual content: A.T.M., A.R.W., V.v.H., G.A. All authors have read and accepted the final version of the manuscript.

## Additional Information

**Supplementary information** accompanies this paper at doi:[10.1038/s41598-017-06387-6](https://doi.org/10.1038/s41598-017-06387-6)

**Competing Interests:** The authors declare that they have no competing interests.

**Publisher's note:** Springer Nature remains neutral with regard to jurisdictional claims in published maps and institutional affiliations.



**Open Access** This article is licensed under a Creative Commons Attribution 4.0 International License, which permits use, sharing, adaptation, distribution and reproduction in any medium or format, as long as you give appropriate credit to the original author(s) and the source, provide a link to the Creative Commons license, and indicate if changes were made. The images or other third party material in this article are included in the article's Creative Commons license, unless indicated otherwise in a credit line to the material. If material is not included in the article's Creative Commons license and your intended use is not permitted by statutory regulation or exceeds the permitted use, you will need to obtain permission directly from the copyright holder. To view a copy of this license, visit <http://creativecommons.org/licenses/by/4.0/>.

© The Author(s) 2017